STUDYING THE FABRICATION OF THIN FILM SILICON SOLAR CELL ON POLYMERIC AND GLASS SUBSTRATE

ANG PUN CHONG

UNIVERSITI SAINS MALAYSIA

2016

STUDYING THE FABRICATION OF THIN FILM SILICON SOLAR CELL ON POLYMERIC AND GLASS SUBSTRATE

by

ANG PUN CHONG

Thesis submitted in fulfillment of the requirements for the degree of

Master of Science

May 2016

ACKNOWLEDGEMENT

Firstly, I would like to express my sincere gratitude to my main supervisor, Professor Kamarulazizi Ibrahim for his valuable guidance and continuous support throughout the course of this project. Besides of guidance and support, your financial assistance from Grant 203/PSF/6721001 is much appreciated.

Thanks to Universiti Sains Malaysia (USM) for giving me this chance to complete my master. Furthermore, technical supports from Nano-Optoelectronics Research and Technology Laboratory (N.O.R) staffs; Mr. Anas, Ms. Ee Bee Choo, Mr. Hazhar Hassan, Mr. Abdul Jamil Yusuf, Mr. Yushamdan and Mr. Aswafi are gratefully acknowledged. Also thanks to my fellow friends; Mohd. Zamir, Ooi Poh Kok, Chai Ying Qi and others (not mentioned here) who have given me useful advices throughout this research.

Finally, I would like to thank my family members for supporting me during the whole research. Not to forget thanks to my girlfriend, Cheng Wei Leng for constant motivation and patience throughout this research and thesis writing process.

TABLE OF CONTENTS

LIST OF TABLES

LIST OF FIGURES

LIST OF ABBREVIATIONS

AFM	Atomic Force Microscopy
AIC	Aluminum Induced Crystallization
AM	Air mass
ARC	Anti-reflection coating
a-Si	Amorphous silicon
ASTM	American Society for Testing and Materials
BSR	Back surface reflector
CB	Conduction band
CIS	Copper indium diselenide
CIGS	Copper indium gallium diselenide
cost/$Watt_p$	Cost per watt peak
c-Si	Monocrystalline silicon
CZ	Czochralski
CZTS	Copper zinc tin sulfide
DC	Direct current
DI	Deionized
DRA	Diffuse reflectance accessories
E-beam	Electron beam
EDX	Energy Dispersive X-Ray
E_g	Band gap
ESRL	Earth System Research Laboratory
eV	Electron volt
FESEM	Field emission scanning electron microscope
FWHM	Full width half maximum
FZ	Float Zone
GW	Gigawatts
HR-XRD	High Resolution X-Ray Diffractometer
ICDD	International Centre for Diffraction Data
IMEC	Interuniversity Microelectronics Centre
IRENA	International Renewable Energy Agency
I-V	Current voltage
LED	Light emitted diode
LPC	Liquid phase crystallization
mc-Si	Multicrystalline silicon
MFC	Mass flow controller
MG-Si	Metallurgical-grade silicon
MHz	Megahertz
NCDC	National Climate Data Center
PET	Polyethylene terephathalate
PI	Polyimide
PL	Photoluminescence
Ppm	Parts per millions
PV	Photovoltaics

PVD	Physical vapor deposition
RF	Radio frequency
RIE	Reactive ion etching
RMS	Root mean square
SIMS	Secondary Ion Mass Spectroscopy
SoG-Si	Solar-grade silicon
SPC	Solid phase crystallization
STC	Standard test condition
TEM	Transmission Electron Microscope
TWh	Terawatts hour
UMG-Si	Upgraded metallurgical-grade silicon
UNSW	University of New South Wales
USD	Dollar America
UV-Vis	Ultraviolet to visible
VB	Valence band

LIST OF SYMBOLS

A	Area of device
A	Absorption
β	Full width half maximum (FWHM) in radians
c	Speed of light
D	Crystal size
E	Energy of photons
FF	Fill factor
h	Planck's constant
Impp	Maximum current
Isc	Short circuit current
Jsc	Short circuit current density
k	Constant value of 0.94
λ	Wavelength
η	Conversion efficiency
Pin	Total illuminated power
P_{mpp}	Maximum power
R	Reflection
R_s	Series resistance
R_{sh}	Shunt resistance
T	Transmission
θ	Bragg's angle
Vmpp	Maximum voltage
Voc	Open circuit voltage

MENGKAJI FABRIKASI FILEM NIPIS SILIKON SEL SURIA DI ATAS SUBSTRAT POLIMER DAN KACA

ABSTRAK

Filem nipis silikon sel suria atas PET substrat difabrikasi dengan mendepositkan filem nipis aluminium (Al) (440nm) sebagai penyambung belakang, filem nipis Al-Si aloi (1 µm) sebagai penyerap, filenm nipis Sb-Si alloy (120nm) sebagai pemancar dan perak (Ag) sebagai penyambung hadapan. Penukaran kecekapan untuk filem nipis silikon sel suria atas PET ialah sekitar 0.105 %. Kecekapan yang rendah ini disebabkan oleh sifat amorfus lapisan penyerap dan pemancar. Untuk mengatasi isu ini, teknik penghabluran aluminium teraruh (AIC) digunakan untuk mencipta filem nipis hablur silikon. Teknik AIC perlu memanaskan sampel sekurang-kurangnya 400 °C, oleh itu PET yang melebur sekitar 250 °C tidak sesuai digunakan sebagai substrat. Substrat PET digantikan dengan substrat kaca dan PI. Struktur untuk filem nipis silicon sel suria di atas kaca dan PI adalah filem nipis tungsten (W) (500 nm) sebagai penyambung belakang, filem nipis Si didopkan dengan Al (ketebalan 180 nm dengan teknik AIC) sebagai lapisan seed dan back surface field (BSF), penebalan epitalesi intrinsik silikon (i-Si) sebagai penyerap, filem nipis zink oksida (ZnO) didopkan dengan galium (Ga) sebagai pemancar dan Ag penyambung hadapan. Filem nipis hablur silikon berjaya dicipta dengan teknik AIC (didopkan secara semula jadi dengan Al dengan kepekatan pendopan sekitar 10^{19} atom/cm^3) di atas substrat kaca dan PI. Keputusan Raman menunjukkan bahawa mereka adalah bersifat hablur dengan puncak Raman (kaca: 520 cm^{-1}, PI: 518 cm^{-1}) iaitu berhampiran puncak Raman c-Si (521 cm^{-1}). Keputusan XRD menunjukkan meraka adalah dalam fasa hablur Si (111). Penebalan epitalesi lapisan biji ini untuk mencipta hablur i-Si

sebagai penyerap juga berjaya dilakukan. Tetapi, qualiti hablur untuk lapisan i-Si adalah sedikit buruk berbanding dengan lapisan biji. Filem nipis ZnO didopkan dengan Ga juga menunjukkan sifat hablur dengan fasa hablur ZnO (002) (mempunyai kepekatan pendopan sekitar 10^{20} atom/cm^3), sifat ini adalah sesuai untuk menjadikan sebagai lapisan pemancar. Penukaran kecekapan untuk filem nipis sel suria di atas substrat kaca dan PI adalah 1.034 % dan 0.924 %.

STUDYING THE FABRICATION OF THIN FILM SILICON SOLAR CELL ON POLYMERIC AND GLASS SUBSTRATE

ABSTRACT

Si thin film solar cell on PET substrate was fabricated by depositing Aluminum (Al) thin film (440 nm) as back contact, Al-Si alloy thin film (1 µm) as absorber layer, Sb-Si allloy thin film (120 nm) as emitter and Silver (Ag) front contact. The final conversion efficiency of the Si thin film solar cell on PET is around 0.105 %. The low efficiency of this device was believed to be cause by the amorphous nature of absorber and emitter layer. In order to solve this issue, fabrication of crystalline Si thin film by Aluminum Induced Crystallization (AIC) technique and SF_6/Ar plasma etch methods were implemented. AIC technique needed to anneal the sample at least to 400 °C, therefore PET which melts at around 250 °C is not suitable. PET substrate was replaced by glass and PI. The structure of Si thin film solar cell for both glass and PI substrate are tungsten (W) thin film (500 nm) as back contact, Al doped Si thin film (180 nm by AIC) as seed layer and back surface field (BSF), epitaxial thickening intrinsic Si (i-Si) as absorber, gallium (Ga) doped zinc oxide (ZnO) thin film as emitter and Ag front contact. Crystallize Si thin film by AIC technique (with naturally Al doped of concentration about 10^{19} atoms/cm^3) was successfully fabricated on both glass and PI substrate. Raman results shows that the sample are crystalline nature with Raman peaks (Glass: 520 cm^{-1}, PI: 518 cm^{-1}) close to Raman peak for c-Si (521 cm^{-1}). XRD spectra shows they are in Si (111) crystalline phase. Epitaxial thickening of this seed layer to create a crystallize i-Si absorber layer is successfully done. However the crystalline quality of i-Si layer is slightly worst compare to seed layer. Sputtered Ga doped ZnO thin film also shown a crystalline nature with ZnO (002) crystalline phase

with doping concentration of around 10^{20} atoms/cm^3, which is suitable for emitter layer. The final conversion efficiency of Si thin film solar cell on glass and PI increased to 1.034 % and 0.924 %.

CHAPTER 1

INTRODUCTION

1.1 Photovoltaics Technologies

Photovoltaics technologies are classified into three major categories, which are: 1) first generation monocrystalline (c-Si) and multicrystalline (mc-Si) wafer-based Si solar cells; 2) second generation thin film based solar cells; 3) third generation high efficiency thin film solar cells.

Nowadays most of the commercial solar cells in the market are based on silicon wafer, which are described as first generation technology. The first generation c-Si and mc-Si wafer-based solar cells exhibit high efficiency (17 - 22%). However, the manufacturing costs for these types of solar cells are relatively high. The high manufacturing cost was due to the high purity c-Si and mc-Si wafers which was produced by Czochralski (CZ), Float Zone (FZ) and casting or directional solidification processes (Mahajan and Harsha, 1999). The current module costs for the first generation solar cells is less than USD$ 1.4/Watt. (IRENA, 2013). The lowest limit of the costs of this generation was predicted to be as low as USD$ 1/Watt (Green, 2003).

The second generation solar cells were based on thin film technology which were deposited on foreign substrates such as glass, plastic and metal sheet. This technology generally includes three major families, which are: 1) thin film Silicon-based such as amorphous silicon (a-Si) and multicrystalline silicon (mc-Si); 2) cadmium telluride (CdTe); 3) copper indium diselenide (CIS), copper indium gallium diselenide (CIGS) and copper zinc tin sulfide (CZTS). Si thin films based solar cells

have more advantages compared to other family due to its stability, manufacturability and abundance. Si thin films based solar cells can avoid resource availability issue which was related to Te and In (Green, 2009). Furthermore, Si is the most abundant element in earth crust after Oxygen (O_2) gas (Green, 2006). The conversion efficiency for second generation solar cells are around 5 to 15%, which is lower compared to Si wafer-based solar cells However, the lower efficiency can be compensated by using the low cost substrate, such as glass and plastic. The overall costs of second generation cells is 2 to 3 times lowers than the cells manufactured from the first generation (Green, 2003).

The third generation solar cells are based on the advanced thin films concepts. Third generation solar cells are not constrained by the efficiency limit of first and second generation, which is 31% under non-concentrated sunlight (Green, 1994). The expected efficiency limit of this generation is as high as 74 % under non-concentrated sunlight (Farrell and Ekins-Daukes, 2011). With the high efficiency conversion, the final cost of third generation cells is 2 to 3 times lower than that of second generation cells. The most common type of third generation cell is tandem cell. Tandem cell is the solar cell produced by combination of several solar cells with different band gaps onto one another to become a complete single cell. Besides tandem cell, hot carrier cell, thermophotovoltaic conversion and multiple quantum well solar cells are also classified as the third generation cells (Green, 2001).

Figure 1.1 shows the possible production costs per unit area and the energy conversion efficiency ranges for the three generations of photovoltaics technologies. First generation solar cells are classified as the group of high production costs and moderate efficiency. With the conversion efficiency of around 20 %, the production cost of this generation in the market is around US$ 150/m^2. Second generation thin

films technology has much lower production cost (US$ 30/m^2) but even more modest efficiency (5 to 12 %). Third generation technology offers at least 2 to 3 times higher efficiency than second generation with almost the same production cost.

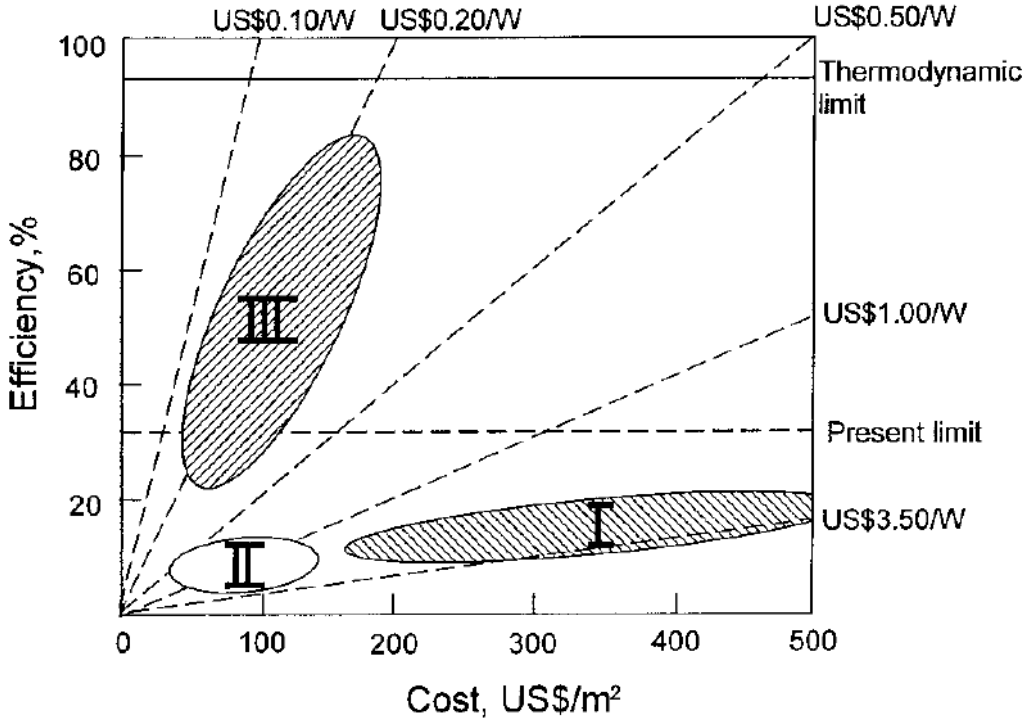

Figure 1.1: Efficiency and cost projections for first, second and third generation photovoltaic technology (Green, 2001).

1.2 Problem Statement

Si is still the preferable material for solar cells fabrication due to its abundance, non-toxicity, good electronic properties and proven reliability (Green, 2000). Furthermore, Si has an optical band gap of 1.12 eV, which is close to the band gap of an ideal photoconverter (1.4 eV) (Nelson, 2003). Owing to these advantages, crystalline Si (c-Si and mc-Si) based solar cells still dominate around 87% of the PV market. Figure 1.2 shows the overall PV market shares in year 2010, which is divided into different technologies (EPIA, 2010).

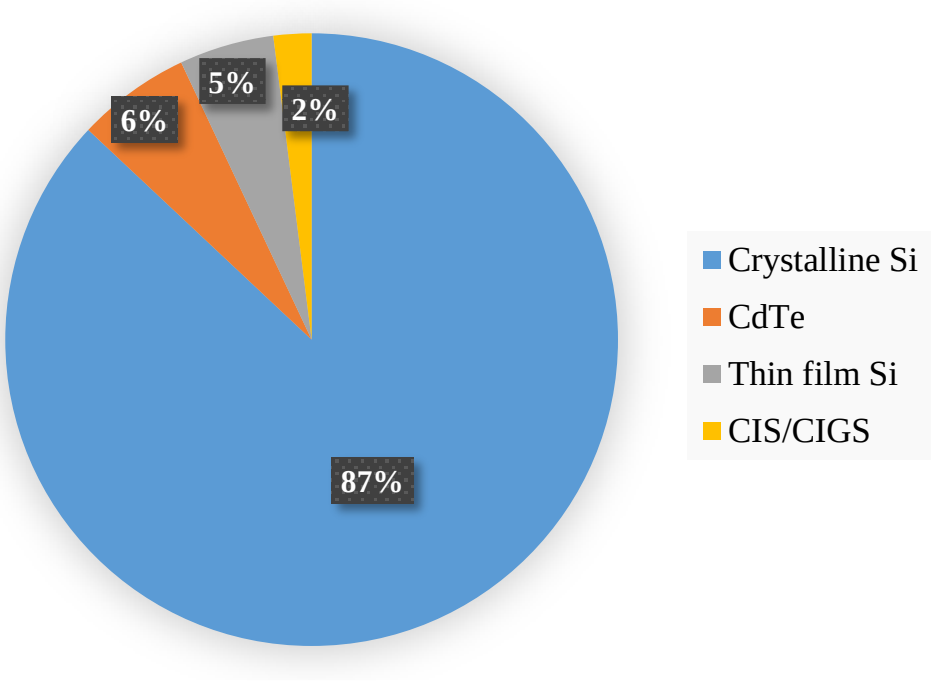

Figure 1.2: Overall PV market shares in year 2010 (divide into different technology).

The main disadvantage for crystalline Si based solar cells is its high manufacturing cost. Low impurity (impurity concentration < 1ppb) and high quality in term of crystal perfection of mono-crystalline Si (c-Si) produced by Czochralski (CZ) and Float-Zone (FZ) techniques prove to yield high efficiency Si solar cells. However, these growth techniques must go through multiple purification steps which make this type of crystalline Si very expensive. Besides of mono-crystalline Si, there is a type of crystalline Si produced via casting and directional solidification technique. This type of crystalline Si called multi-crystalline Si (mc-Si). Production of mc-Si involves lower cost and higher throughput compared to c-Si. Crystalline Si based solar cells produce from mc-Si wafer prove to have around 80 % performance of c-Si wafer based solar cell.

Besides, both of c-Si and mc-Si based solar cells are also highly material-intensive. In order to make sure a complete absorption of incident sunlight, the thickness of the crystalline Si (both c-Si and mc-Si) wafers are fabricated to around

180 to 200 μm. The needs of such high thickness was due to the indirect band gap properties of Si material. This indirect band gap property causes it to be a poor light absorption material (Runyan, 1965). Furthermore, owing to the high cost of raw silicon material, which occupies around 50% of the finished PV module (Rubin, 2010), the production cost of the crystalline Si wafer based solar cells in the market is still high (around USD 2 to 3/$Watt_p$) for large scale manufacturers (Green, 2003).

1.3 Scope of Research

This work will focus on the study of the second generation solar cells. As discussed on the previous section, second generation solar cell is the technology which involves the deposition of thin film semiconductor on the foreign substrate. In this experiment, thin film Si solar cell will be deposited on the foreign substrates via electron beam evaporation method. This is an effective way to reduce the cost/$Watt_p$ of the final solar cells because of the low material consumption.

To reduce material consumption, the thickness of the Si thin film will reduce to 1 – 1.5 μm (150 to 200 times thinner than the thickness of the conventional Si wafer) (Song, 2005). In addition, the cost/$Watt_p$ of the final product can be reduced further by replacing the conventional glass substrate to polymeric type substrate (such as polyethylene terephthalate, PET and polyimide, PI). The cost of polymeric substrate is lower compared to glass substrate, therefore the cost/ $Watt_p$ of the final products can be reduced. Besides, polymeric is also light in weight and highly flexible. These properties make it capable for roll to roll deposition process (Rath et al., 2008). Electron beam evaporation is chosen to be the main deposition method of thin film Si due to its high deposition rate (up to 1 μm/min).

The advantages of low material consumption and low cost polymeric substrate could potentially yield to lower cost/$Watt_p$ thin film Si solar cells with reasonable device conversion efficiency.

1.4 Research Originality

Originality of this research is the fabrication of low cost second generation thin film Si solar cell on flexible polymeric and glass substrate. Low cost can be achieved by much lower material consumption due to thinner structure (150 to 200 times thinner compared to conventional Si wafer based cell). The fabrication method consists e-beam deposition, Aluminum Induced Crystallization (AIC) and Sulfur Hexafluride (SF_6)/Argon (Ar) plasma etch. This fabrication method is rarely reported in literature. In this research, a function crystalline thin film Si solar cell on polymeric and glass substrate can be fabricated at low temperature (400 °C), which leads to the advantage of low energy consumption during the fabrication processes.

1.5 Objectives of Research

The objectives of this work are listed as below:

1. Study the fabrication of thin film Si solar cells on polyethylene terephathalate (PET) substrates via electron beam evaporation.
2. Study the fabrication of thin film Si solar cells on sodalime glass and polyimide (PI) substrates via electron beam evaporation and Aluminum Induced Crystallization (AIC) technique.
3. To compare the performance between the thin film Si solar cells deposited on PET, sodalime glass and PI substrate.

This work does not aim to fabricate high efficiency thin film Si solar cells on PET, sodalime glass and PI substrates, but rather to understand the underlying factors which affect the performance of the devices.

1.6 Thesis Outline

Chapter 1 explains the solar energy, photovoltaics technologies and problem statement. Scope and objectives of this research are also discussed in this chapter.

Chapter 2 briefly goes through the thin film solar cells. Discussed issues and approach in thin film Si solar cell research.

Chapter 3 presents basic of relevant theories such as solar spectrum, properties of Si, doping of Si, PN junction, PIN junction, Current-Voltage characteristic and efficiency calculation.

Chapter 4 presents the material and methods needed for the fabrication of thin film Si solar cell on polymeric and glass substrate. This includes the deposition equipment, annealing equipment and several types of characterization equipment. Besides, the detail of fabrication process steps for Si thin film solar cell on polymeric and glass substrate will be explained.

Chapter 5 illustrates the experimental results, calculations, explains and discuss the observations and finding.

Chapter 6 summarizes the overall findings and lists some recommendations for future works on thin film Si solar cell fabrication on polymeric and glass substrate.

CHAPTER 2

LITERATURE REVIEW

2.1 Introduction

This chapter will go through the basic of thin film solar cells and the types of thin film solar cells technologies. Besides, the thin film solar cells issues, such as weak absorption of Si and high recombination at defects will also be studied. Finally, the progress of thin film solar cells researches by Photovoltaics Centre of Excellence, University of New South Wales (UNSW) and Interuniversity Microelectronics Centre (IMEC) will be shown in this chapter.

2.2 Thin Film Solar Cells

Thin film solar cells or the second generation solar cells which fabrication is performed by depositing multiple layers or thin films of photovoltaic material onto a foreign substrate. The material of the substrate can be stainless steels, glasses or flexible plastic materials. Currently, there are few types of thin film technologies, such as amorphous silicon (a-Si), microcrystalline silicon (μc-Si), polycrystalline silicon (pc-Si), cadmium telluride (CdTe), copper indium diselenide (CIS), copper indium gallium diselenide (CIGS), copper zinc tin sulfide (CZTS) and polymer based solar cells (Shah et al., 2004). The thin film solar cells are typically deposited via chemical vapour deposition (CVD), physical vapour deposition (PVD), electrochemical and spin-on methods onto a foreign substrate. The substrate is used to improve the mechanical strengths. Thin film solar cells have advantage of fairly high optical absorption (especially for CdTe and CIGS), however, its minority carrier diffusion

lengths is fairly low due to the presence of defects and grain boundaries. Normally, thin film solar cells have low conversion efficiencies (5 – 15%) but with two to three times lower production costs compared to the first generation cells (Nelson, 2003).

2.3 Issues of Thin Film Si Solar Cells Research

Thin film Si solar cell technology believes to be one of the effective approaches which leads to the reduction of the total manufacturing cost of solar cells. However, there are several issues that need to be solved.

The main issue is the weak light absorption material of Si (especially at near infrared region) at low thickness. It is due to the fact that Si is an indirect band gap semiconductor (Brendel, 2005). In order to solve this problem, light trapping strategy is applied within the structure of thin film solar cells. The advantage of light trapping strategy is to increase optical path length of photon within the solar cell which leads to higher potential of photon absorption and directly increases the photocurrent generation (Cho et al., 2011). Besides, the light trapping strategy can be improved by incorporating of several thin film deposition, such as anti-reflection coating (ARC) (usually Si_xN_y, ZnO, SiO_2 or ITO) (Yang et al., 2011). Furthermore, deposition of a back surface reflector (BSR) layer at the back surface of solar cells is also an effective approach to trap more photons. There are several types of BSR, they are metal, dielectric or multilayer porous or a silver (Ag) plasmonics nanostructures (Sai et al., 2009, Pillai and Green, 2010).

High recombination of electron-hole pairs at defects is another issue that need to be solved. There are several types of defects in Si thin film, they are lattice mismatch, grains boundaries and dangling bonds. These types of defects will act as effective trap states and recombination centres to electron-hole pairs (Mahajan and Harsha, 1999).

Normally, the defects are created due to contamination of impurities into Si atoms during deposition of Si thin film. Besides, defects can also be created by structural imperfection within the Si thin film which is generated during deposition.

The issue of high recombination at defects can be solved by depositing the thin film Si in a high vacuum environment. One of the high vacuum deposition methods is e-beam evaporation. Typically, the base pressure of e-beam evaporation chamber can go up to > 10^{-8} Torr and deposition pressure of > 10^{-7} Torr. E-beam evaporation is simple and attractive due to its high deposition rate (up to 1 μm/min) (Kunz et al., 2009). In additions, high temperature deposition process or low temperature deposition process with further treatment of high annealing temperature to produce large grains absorber and defects annealing are also the methods to solve this issue (Rau et al., 2009). Recently, liquid phase crystallization (LPC) is proved to be able to produce a high quality crystalline Si thin film on glass. These types of Si thin films have low defect density, high carrier motilities, and high minority carrier lifetime of over 260 ns (Varlamov et al., 2013).

2.4 Progress in Thin Film Silicon Solar Cells Research (Methods and Approaches)

There are two main groups of researchers have done extensive research in thin film Si solar cells. They are Photovoltaics Centre of Excellence, University of New South Wales (UNSW) and Interuniversity Microelectronics Centre (IMEC).

Researchers in UNSW focuses on the study of pc-Si thin film solar cells on borosilicate glass. Three different types of pc-Si thin film solar cells have been developed, which are EVA, ALICE and ALICIA (Aberle, 2006b). Figure 2.1 shows the process steps of EVA, ALICE and ALICIA.

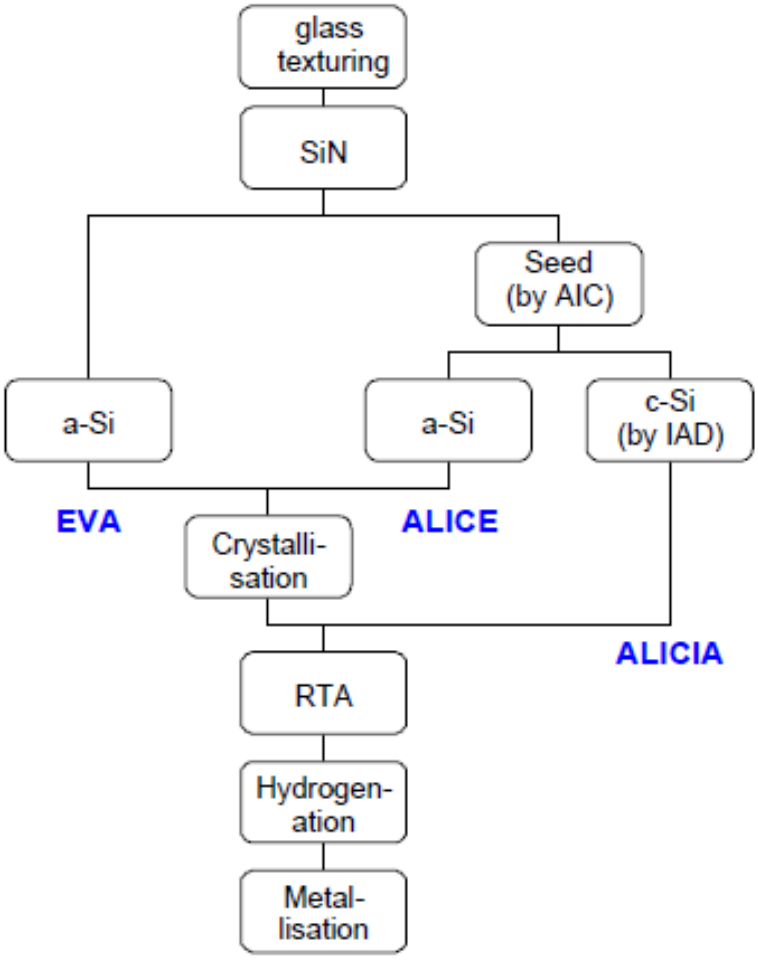

Figure 2.1: Process steps of EVA, ALICE and ALICIA solar cell (Aberle, 2006b).

The substrate used in these works are borosilicate glass with thickness of 3 mm. All the devices are designed in superstrate structure where the substrate is faced to the sunlight, which is opposite to the conventional structure. For the first steps, texturing of glass substrate is performed by aluminum induced texture (AIT) (Chuansuwanich et al., 2005). AIT creates a random sub-micron sized of dimples on glass surface. AIT technique is performed by depositing a thin film Al with thickness of about 50 nm on to the glass substrate and followed by thermal annealing at about 600°C for 30 minutes. Then, the thin film Al is etched off by wet-chemical etching.

The main advantages of evaporated (EVA) solar cell is their simplicity where no seed layer is included. However, its solar cell's performance is limited due to the

relatively small grain size (normally in range of 1 – 2 μm), which affects its electrical performance caused by the grain boundaries effects. EVA Si thin film solar cell on borosilicate glass substrate with conversion efficiency of 4 % is successfully fabricated (Kunz et al., 2008). The schematic structure of the EVA solar cell is shown as Figure 2.2.

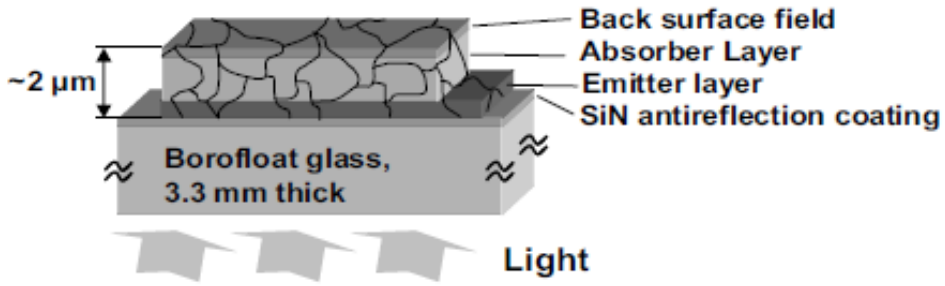

Figure 2.2: Schematic structure of the EVA solar cell (Kunz et al., 2008).

An antireflection coating (ARC) of Silicon Nitride (SiN) layer was firstly deposited onto the borosilicate glass substrate. The ARC layer serves as both antireflection coating and barrier layer for contaminations from substrate. ARC layer can be deposited by plasma enhanced chemical vapor deposition (PECVD) or sputtering. After that, the combination layers of a-Si thin film emitter, absorber and back surface field (BSF) layer are deposited by electron beam (e-beam) evaporation under high vacuum (base pressure around 2×10^{-8} Torr; working pressure around 2×10^{-7} Torr). The total thickness of these three layers are controlled within around 2 μm. Then, the sample will go through solid phase crystallization (SPC) and rapid thermal annealing (RTA). After RTA process, the sample was exposed to hydrogen plasma treatment. The details of parameters for EVA solar cell fabrication is shown in Table 2.1.

Table 2.1: Details of parameters for EVA solar cell fabrication (Kunz et al., 2008).

Parameter	Details
Glass	3.3 mm, borosilicate, planar or textured
AR coating	~ 70 nm, SiN, $n \approx 2.1$
Emitter	~ 100 nm, p^+ or n^+, ~ 200-400 Ω/sq
Base	~ 1.8 μm, n^- or p^-, ~ 5×10^{16} cm^{-3}
BSF	~ 100 nm, n^+ or p^+, ~ 500-1000 Ω/sq
SPC	≥ 24h at 600°C
RTA	4 min at ~900°C
Hydrogenation	15-20 min at ~ 600-650°C, remote plasma

For ALICE and ALICIA solar cell, both of them are fabricated by deposition of epitaxial thickening of Si absorber layer on Aluminum Induced Crystallization (AIC) seed layer. The seed layer is formed by thermally annealed a-Si and Al bilayers at 500 °C. The epitaxial thickening layer of ALICE cells is deposited by e-beam evaporation followed with SPC process (or called Solid Phase Epitaxy, SPE) (Widenborg et al., 2005), which is the same process as EVA cell. For ALICIA cell, the epitaxial thickening layer is deposited by Ion Assisted Deposition (IAD) (Aberle et al., 2005).

Table 2.2 shows the typical parameter for an ALICE and ALICIA cells. The emitter layer of around 150 nm with doping concentration of nearly 1×10^{19} cm^{-3} is fabricated by AIC technique. AIC technique proved that a well crystalline Si thin film can be fabricated by stacking a-Si layer with Al layer and annealed below the eutectic temperature (577 °C) (Nast et al., 1998, Nast et al., 2001).

Table 2.2: Typical parameter for an ALICE and ALICIA cells (Aberle, 2006b).

Parameter	Details
Glass	3 mm (planar or textured, borosilicate)
AR coating	SiN (~75 nm, refractive index ~2.0)
Emitter	p^+ (~150 nm, ~1×10^{19} cm^{-3} Al+B, ~1000 Ω/sq)
Base	n (~1500 nm, ~5×10^{16} cm^{-3} P)
BSF	n^+ (~100 nm, ~1×10^{19} cm^{-3} P, ~1000 Ω/sq)
RTA	10 s at 1000°C or 4 min at 900°C
Hydrogenation	~15 min at 620°C, remote plasma
Metallisation	Al (500 nm, front & rear)

Figure 2.3 shows the cross section TEM image of an ALICIA cell. The figure illustrates a good transfer of crystalline quality from seed layer produced by AIC to the epitaxial thickening absorber layer.

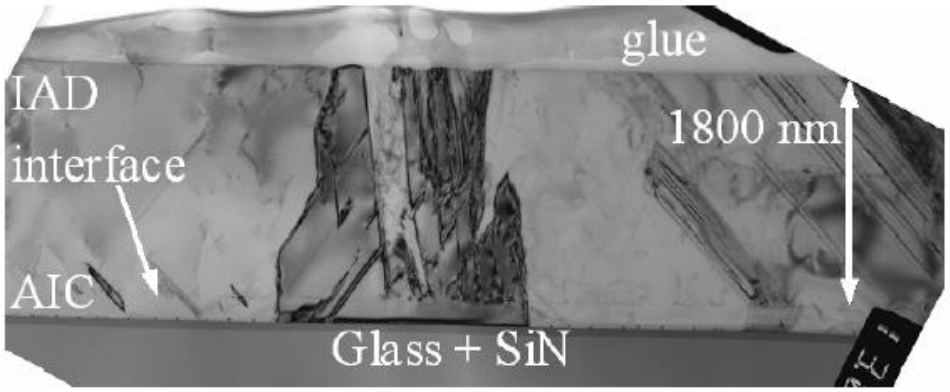

Figure 2.3: Cross section TEM image of an ALICIA cell (Varlamov et al., 2013).

Besides of the SPC and AIC crystallization technique, UNSW research team members have invented a new crystallization technique called liquid phase crystallization (LPC) technique. This technique proved to have Si thin film with grain size up to millimeter (mm) scale. The highest conversion efficiency of Si thin film solar cell achieved by LPC technique is 11.7 % (Varlamov et al., 2013). LPC of Si thin film is performed by line-focus laser crystallization. Figure 2.4 shows the photo of

line-focus laser crystallization technique, the resulting grain size is shown in TEM image (attached in Figure 2.4).

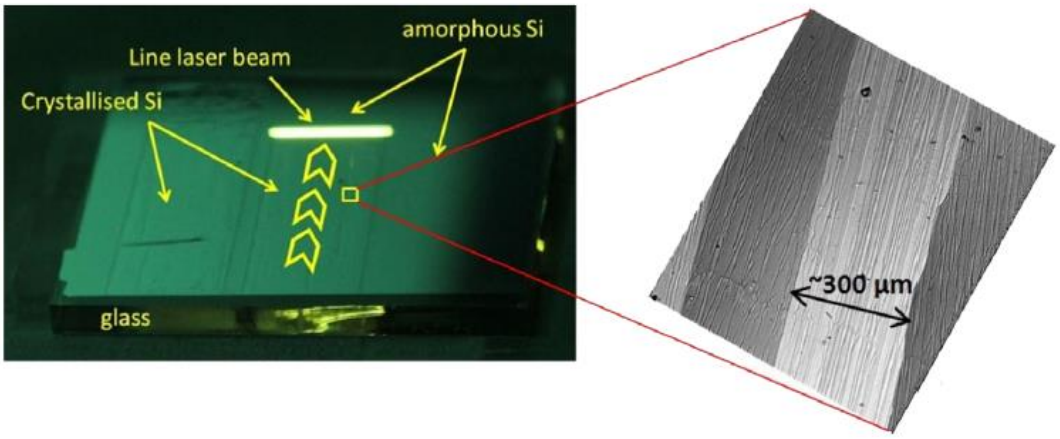

Figure 2.4: Photo of line-focus laser crystallization technique attached with TEM image (Varlamov et al., 2013).

IMEC research team has also done a massive research in Si thin film solar cells fabricated by AIC seed layer concepts. Si thin film solar cell on alumina substrate with the efficiency of 4.5% was achieved by them using AIC seed layer concept with epitaxial thickening of absorber layer (Gordon et al., 2005). The seed layer is fabricated by depositing a bi-layer of a-Si and Al thin film (200 nm and 230 nm respectively) onto an alumina substrate using e-beam evaporation. After deposition, the samples are annealed in tube furnace with temperature at 500 °C (under N_2 ambient for 0.5 to 3 hours). The top Al layer is then removed by Al selective etchants. Si epitaxial thickening layer is deposited on the seed layer by commercial single-wafer epitaxial reactor (ASM Epsilon 2000) using trichlorosilane diluted in H_2 at 1130 °C (under atmospheric pressure). The in situ boron (B) doping is performed by adding the flow of diborane gas (Gordon et al., 2005).

IMEC research team successfully fabricated Si thin film solar cell on alumina substrate with conversion efficiency of 8.0 %. The cell is also fabricated by means of

AIC seed layer with epitaxial thickening absorber layer. There is an addition of improvement step which is the plasma texturing of absorber layer with hexaflurosilane (SiF_6) and nitrous oxide (N_2O) gases (Gordon, et al., 2007). Figure 2.5 shows the schematic drawing of IMEC's Si thin film solar cell.

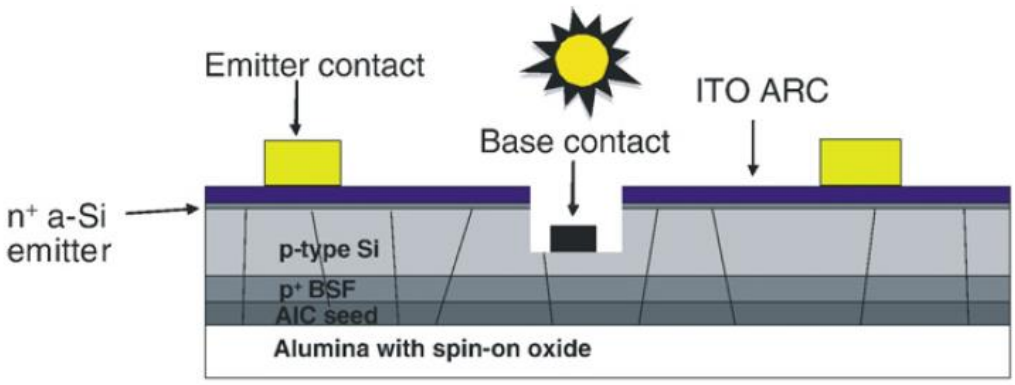

Figure 2.5: Schematic drawing of IMEC's Si thin film solar cell (Gordon, et al., 2007).

Fabrication of Si thin film solar cell via e-beam evaporation and AIC technique on low cost polymeric substrate and lower grade sodalime glass are hardly reported in the literature. One of the reasons is due to its relatively low quality of crystalline Si. In this research, a-Si thin film solar cell is fabricated on low cost polyethylene terephthalate (PET) substrate via e-beam co-evaporation technique. In additions, the structure is improved by fabrication of crystallize Si thin film solar cells on polyimide (PI) and sodalime glass substrate by means of AIC technique with epitaxial thickening of absorber layer.

CHAPTER 3

THEORY

3.1 Introduction

This chapter will go through a brief introduction of solar spectrum (AM 1.5 Global) and properties of silicon material which included doping of silicon and absorption coefficient of silicon. The basic formation of PN and PIN junction will also be studied in this chapter. Lastly, the electrical characteristic of solar cells such as equivalent circuit and current-voltage characteristic of solar cells will be shown.

3.2 Solar Spectrum

Figure 3.1 shows the solar irradiance (Air Mass, AM 1.5 Global) of sun range from wavelength of 200 nm to 2500 nm (from ASTM G173-03 reference spectral) (ASTM, 2008). This is the spectral for terrestrial use, which has an integrated power of 1000 W/m^2.

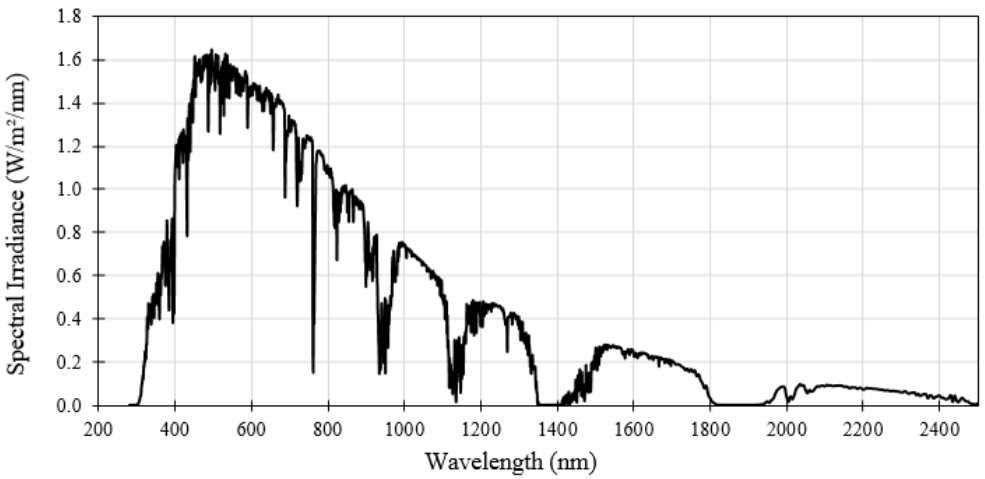

Figure 3.1: Spectral irradiance of sun under AM 1.5 Global (Nelson, 2003).

Air Mass (AM) shows the optical path length of sunlight which need to pass through before it reaches the surface of earth. AM value determined the total reduction of sunlight's power as it pass through the atmosphere. The power reduction is due to the absorption by air and dust. The AM value is calculated by AM = 1/cos (φ), where φ is the angle from the vertical line (zenith angle). For AM 1.5, the φ angle is equal to 48.2°. AM 1.5 Global is the standard test condition (STC) for solar cell's current-voltage (I-V) characterizations (Nelson, 2003).

3.3 Properties of Silicon Material

Silicon is a semiconductor material with chemical symbol Si and atomic number 14 (electronic configuration: 2, 8, 4). It is a group IV element in periodic table with 4 valence electrons. Si is a solid material under room temperature with relatively high melting point (1414 °C) and boiling point (3265 °C). It crystallizes in a diamond cubic crystal structure with lattice spacing of 0.5431 nm. Crystalline Si has a gray metallic color and very brittle.

Si is chosen as the main material for solar cells fabrication due to its abundance, non-toxicity, proven durability and good electronic properties (Green, 1995). Si is the most abundant element in earth crust beside Oxygen, O_2. There is about 25 % of silica can be found in earth crust. Besides, Si has a band gap (E_g) of 1.12 eV at room temperature, which is close to the ideal band gap of a photocenverter (around 1.4 eV) (Nelson, 2003).

For Si material, the valence band (VB) and conduction band (CB) are separated by a forbidden gap called band gap (E_g) of 1.12 eV. Electrons are tightly bond and not freely to move in VB, in order to move freely it must be excited to CB. In Si material,

minimum energy required to excite an electron from VB to CB is 1.12 eV (E_g for Si). Photons which carry the energy of around 1.12 eV can be calculate by formula below,

$E = hc/\lambda$

where,

E = Energy of photons in electron volts (eV)

h = Planck's constant, 4.1357×10^{-15} eV.s

c = Speed of light, 3×10^{8} m/s

λ = wavelength of light in nm

From the formula above, photons of wavelength about 1100 nm carry energy of around 1.12 eV. Therefore, Si needed to absorb photons with wavelength of 1100 nm and below to create free electrons and produce photocurrent.

3.4 Doping of Silicon

Doping of silicon is a technique of introducing selected impurities into pure (intrinsic) silicon for the purpose of modify its electrical properties. There are two types of doped Si, which are p-type Si and n-type Si. Doping of Si results one less electron (hole) known as p-type Si.

Introducing group 3 element (tetravalent atom) such as boron (B) or aluminum (Al) results extra of holes as the majority carriers in Si which called a p-type doped Si. For n-type doped Si, group 5 element (pentavalent atoms) such as phosphorus (P), antimony (Sb) and arsenic (As) need to introduce in to intrinsic Si lattice which produces extra of electrons as the majority carriers in Si lattice. Figure 3.2 shows the schematic of p-type and n-type doped Si crystal lattice.

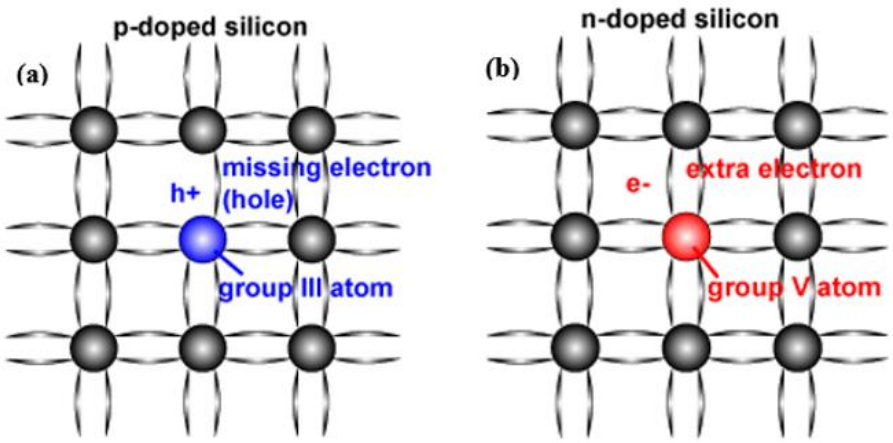

Figure 3.2: Schematic of (a) p-type doped and (b) n-type doped Si crystal lattice (Honsberg and Bowden, 2010).

The Fermi energy (E_F) level in an intrinsic Si will shifted due to doping. For intrinsic Si, E_F level is approximately in the middle of valence band (VB) and conduction band (CB) or half of band gap ($E_g/2$). On the other hand, the E_F level for p-type doped Si is shift towards VB edge. However, E_F level for n-type doped Si is shift towards CB edge. The schematic for the positon of E_F level for intrinsic, p-type doped and n-type doped Si are shown in Figure 3.3.

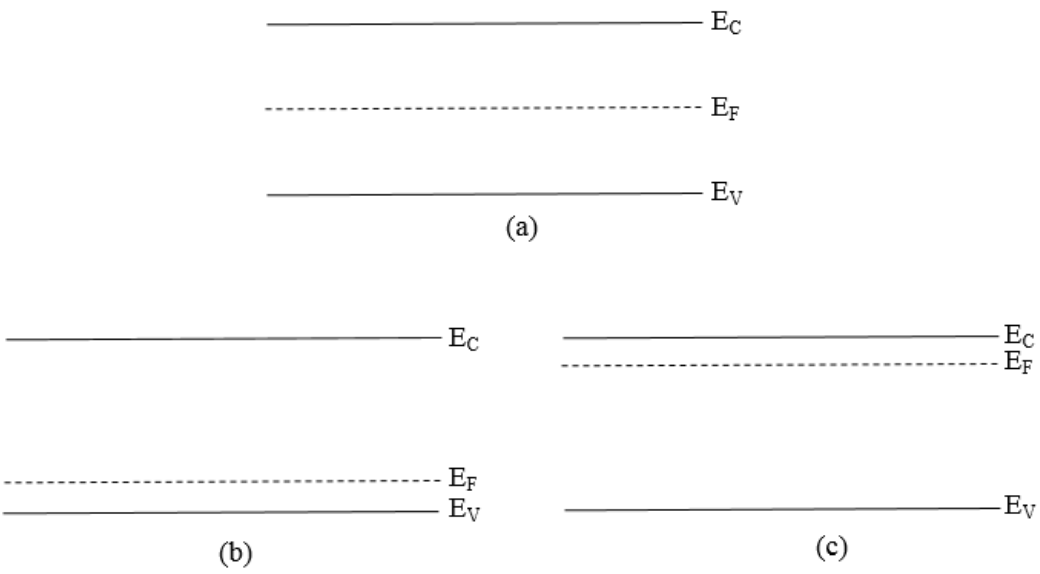

Figure 3.3: Schematic for the positon of E_F level for (a) intrinsic, (b) p-type doped and (c) n-type doped Si (Nelson, 2003).

3.5 Absorption Coefficient of Silicon

Figure 3.4 shows the plot of absorption coefficient (α, in logarithmic scale) of various semiconductor materials at temperature of 300 K versus wavelength (nm). Absorption coefficient measures how far distance into a particular material that light of a particular wavelength can penetrate before it is absorbed. Material with high absorption coefficient absorb the light stronger compared to material with low absorption coefficient.

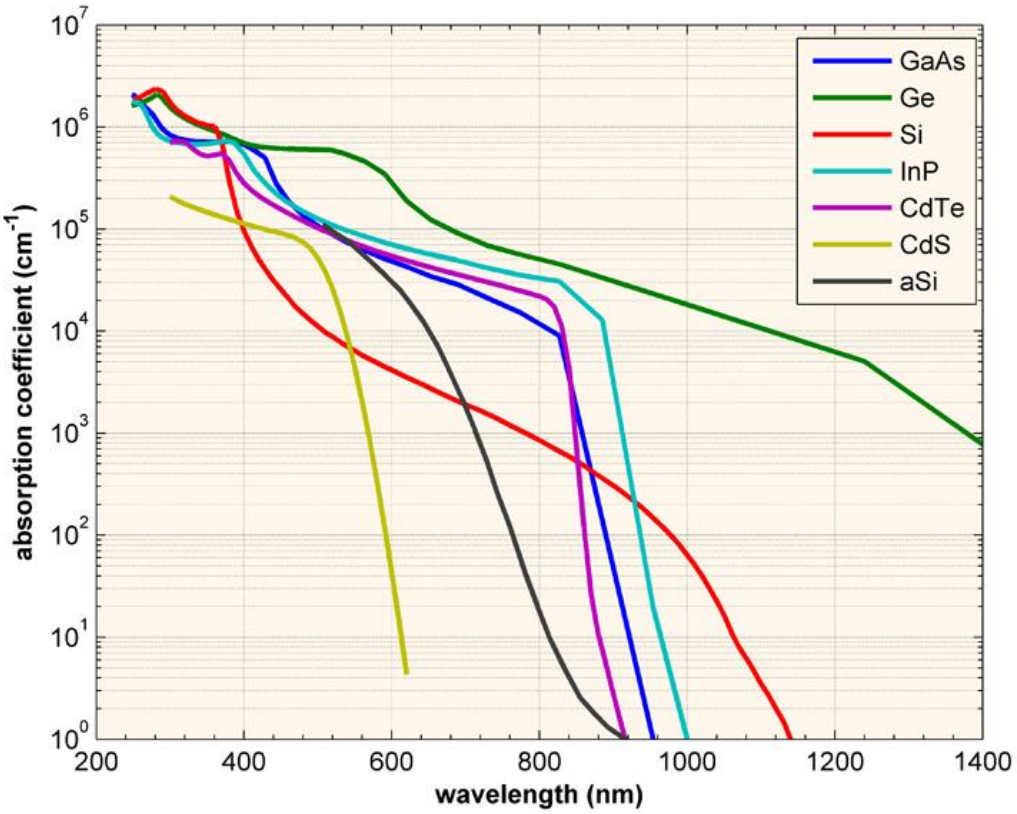

Figure 3.4: Plot of absorption coefficient (α, in logarithmic scale) of various semiconductor materials at 300 K versus wavelength (nm) (Honsberg and Bowden, 2010).

From Figure 3.4, it can be seen that all semiconductor material have a sharp transition edges at their respective band gaps. This phenomenon was due to the photons with energy lower than the band gap (Eph < Eg) do not have sufficient energy to excite an electron from valence band to conduction band.

In additions, Figure 3.4 shows that Si has a slower transition in its absorption profile compared to other material like GaAs, CdTe, CdS, InP and a-Si. This is due to Si is an indirect material while GaAs, CdTe, CdS, InP and a-Si are direct band gap materials. Direct band gap materials generally have higher ability in optical absorption compared to indirect band gap material (Nelson, 2003). An indirect band gap material (i.e. Si) requires assistance from phonons with the right momentum (k) to enable electron transition from valence band (VB) to conduction band (CB), therefore its optical absorption is weaker compared to material with direct band gap. Comparison in band structure of direct and indirect band gap material is shown in Figure 3.5.

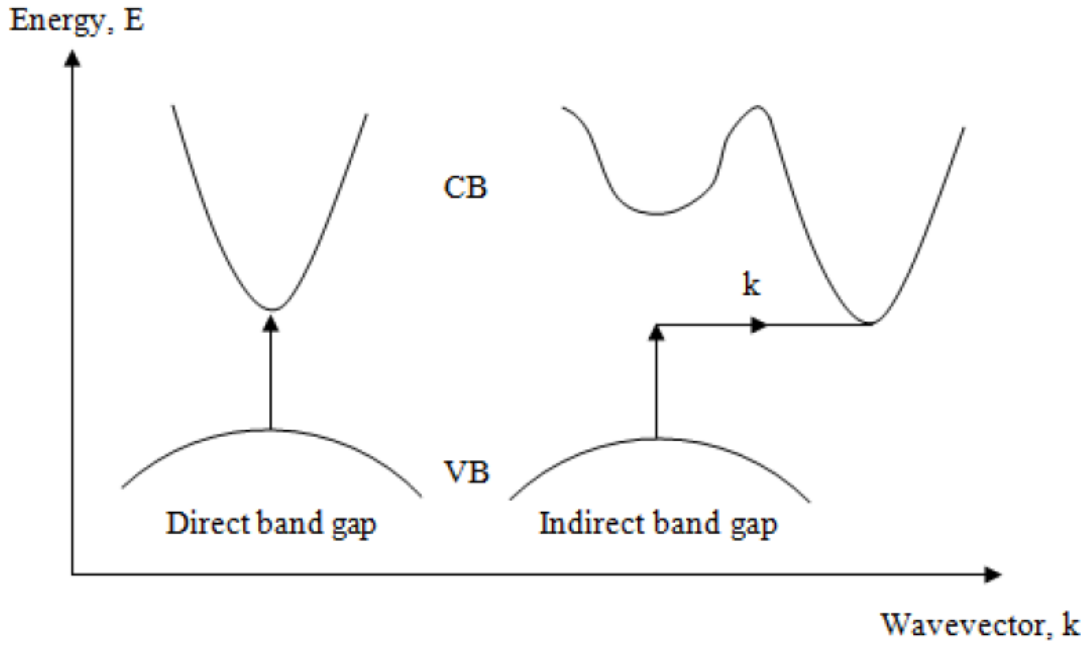

Figure 3.5: Band structure of direct and indirect band gap material (Nelson, 2003).

3.6 PN Junction and PIN Junction Formation

Figure 3.6 shows the schematic diagram and energy band diagram for a PN junction. PN junction is formed by joining p-type doped Si with n-type doped Si. P-type region has high holes concentration while n-type region has high electrons concentration. When both of these material joining together, holes from p-type region will diffuse to n-type region and electrons from n-type region will diffuse p-type region due to concentration gradient at the junction. However, the diffusion process is altered by formation of an internal electric field. This internal electric field is formed when the electrons and holes move to the other side of the junction, they leave behind exposed charges (negative charge on p-type region and positive charge on n-type region).

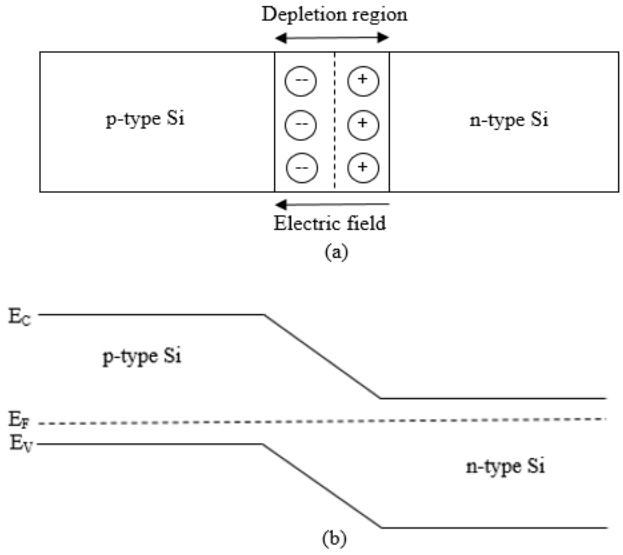

Figure 3.6: (a) Schematic diagram of a PN junction (b) Band diagram of a PN junction (Nelson, 2003).

The PN junction is the core structure for a solar cell devices. PN junction serves as a barrier to majority carriers and low resistance path for minority carriers. The main function of the PN junction is to drive the collection of minority carriers which are

photogenerated throughout p-type and n-type region to reach junction via diffusion and drift (Nelson, 2003).

Figure 3.7 shows the schematic diagram and energy band diagram for a PIN junction. PIN junction is formed where an intrinsic (undoped) Si layer is sandwiched between p-type doped and n-type doped Si layer. The internal electric field is formed at the junction or between the p-type doped and n-type doped layer, but the region is extends wider due to the inclusion of intrinsic layer (Green, 1982).

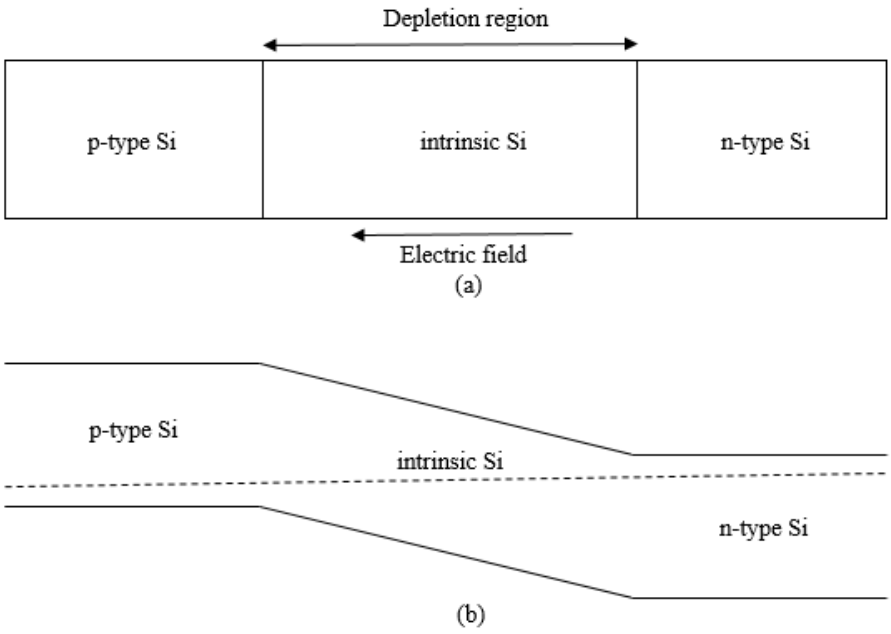

Figure 3.7: (a) Schematic diagram of a PIN junction (b) Band diagram of a PIN junction (Nelson, 2003).

This structure is not preferred for thin film solar cells fabrication due to its imperfect lattice formation resulting from various deposition technique. This lattice imperfection directly causes the decreases of minority carrier diffusion length. For PIN structure, p-type and n-type doped layer is generally not contribute to the photogenerated current. Carriers are mainly generated within the intrinsic layer and drive towards the p-type and n-type doped layer by the internal electric field (Nelson, 2003).